Int. J. Electrochem. Sci., 8 **(2013)** 7030 - 7043

International Journal of
ELECTROCHEMICAL
SCIENCE
www.electrochemsci.org

Electrochemical Analysis of the Performance of Carbon Supported Pd Nanoparticles for Direct Formic Acid Fuel Cells: From Gold Supported Electrodes to Catalyst-Coated Membranes

Alfonso Sáez, José Solla-Gullón, Eduardo Expósito, Antonio Aldaz, Vicente Montiel[*]

Departamento de Química-Física e Instituto de Electroquímica. Universidad de Alicante. Apartado 99, 03080 Alicante. Spain.
[*]E-mail: vicente.montiel@ua.es

Received: 18 December 2012 / *Accepted:* 21 March 2013 / *Published:* 1 May 2013

In this work carbon supported Pd nanoparticles were prepared and used as electrocatalysts for formic acid electrooxidation fuel cells. The influence of some relevant parameters such as the nominal Pt loading, the Nafion/total solids ratio as well as the Pd loading towards formic acid electrooxidation was evaluated using gold supported catalytic layer electrodes which were prepared using a similar methodology to that employed in the preparation of conventional catalyst coated membranes (CCM). The results obtained show that, for constant Pd loading, the nominal Pd loading and the Nafion percentage on the catalytic layer do not play an important role on the resulting electrocatalytic properties. The main parameter affecting the electrocatalytic activity of the electrodes seems to be the Pd loading, although the resulting activity is not directly proportional to the increased Pd loading. Thus, whereas the Pd loading is multiplied by a factor of 10, the activity is only twice which evidences an important decrease in the Pd utilization. In fact, the results obtained suggest the active layer is the outer one being clearly independent of the catalytic layer thickness. Finally, catalyst coated membranes with Pd catalyst loadings of 0.1, 0.5 and 1.2 mg cm^{-2} were also tested in a breathing direct formic acid fuel cell.

Keywords: Pd/C, Gold supported working electrodes, CCM, DFAFC

1. INTRODUCTION

Formic acid oxidation is one of the most studied electrochemical reactions due to its interest in fuel cells. In this sense, formic acid is being considered as a substitute for methanol as fuel in direct liquid fuel cells [1-4]. As it is well known whereas methanol has a number of drawbacks such as crossover through the membrane that causes a decrease in catalytic activity or certain environmental

considerations due to its toxicity, formic acid is classified as non-toxic and also its crossover is considerably much lower than methanol thus allowing using higher formic acid concentrations, which increases the efficiency of the stack.

On the other hand, the electrooxidation mechanism of formic acid is considered a model reaction, as it provides a simplified example of the oxidation of more complex organic molecules that can also be used in this field. Formic acid oxidation takes place through a widely accepted dual path mechanism; one leading to the direct formation of CO_2 and the poisoning path, which involves a dehydration step to yield water and adsorbed CO and its further oxidation to CO_2 at high potentials [5, 6]. According to this mechanism, it is well known that the rate of formic acid oxidation is strongly affected by the spontaneous formation of the poison through the dehydration step of the formic acid molecule to yield CO. Consequently, it is important to find catalysts able to directly oxidise formic acid to CO_2 in which the poison-mediated contribution was minimum.

In this regard, it is well established that palladium is a very interesting choice [7, 8]. Pd exhibits a better electrocatalytic activity towards formic acid oxidation than Pt. There are two main reasons for that: i) Unlike platinum, no CO is formed, and therefore the reaction takes place through the direct path (1) and ii) the onset potential for the oxidation is ca. 200 mV lower [3, 4, 9, 10]:

$$HCOOH \rightarrow \text{Active Intermediate} \rightarrow CO_2 \quad (1)$$

On the other hand, it should also be taken into account that a membrane fuel cell is a complex system, even when using a laboratory scale single cell unit. In previous contributions, we have reported that the use of gold supported catalytic layer electrodes [11, 12], prepared using a similar methodology to that employed in the preparation of conventional catalyst coated membranes, allows obtaining not only electrodes with comparable properties, in terms of morphology and thickness, than those employed in real direct liquid fuel cell systems but also allowing an easier electrochemical characterization of those experimental parameters that may affect its electrochemical behaviour such as percentage of metal in the catalyst, Nafion (ionomer) / total solids ratio, catalyst loading, among others.

In this way, the main objective of the present paper is to perform a complete electrochemical study of the experimental parameter affecting the behaviour of carbon supported Pd nanoparticles towards formic acid electrooxidation using home-made gold supported catalytic layers build with similar characteristics (morphology and thickness) than those found in a direct liquid fuel cell. Finally, catalyst coated membranes (CCM) were also prepared and tested in a breathing direct formic acid fuel cell.

2. EXPERIMENTAL PART

2.1. Synthesis of electrocatalysts and fabrication of working electrodes.

Pd nanoparticles supported on Vulcan XC-72 were synthesized by reducing K_2PdCl_4 with $NaBH_4$ using a water-in-oil (w/o) microemulsion of water (3 %)/polyethylene glycol dodecyl ether

(BRIJ®30) (16.5 %)/n-heptane (80.5 %) following a similar methodology to that already reported in previous works [13]. The values in brackets represent the volume percentage of each compound. The synthesis was performed by directly adding $NaBH_4$ to the micellar solution. The concentration of the K_2PdCl_4 in the water phase was 0.1 M and the sodium borohydride was added as a solid. The total amount of $NaBH_4$ was ten times the stoichiometric amount. After the reduction step, the carbon Vulcan XC-72 was added under fast stirring, alternating both magnetic and ultrasonic for about 1 h, in order to properly disperse the nanoparticles on the carbon support. Different nominal Pd loadings (10, 20 30 and 40% wt) were obtained by simply varying the ratio between amount of Pd and carbon Vulcan XC-72 in the synthesis solution. Once the nanoparticles were dispersed on the carbon surface, acetone was added to the mixture to cause phase separation which also induces a complete precipitation of the solid. After complete precipitation, the sample was filtered, cleaned employing the protocol previously described [13], and finally dried at 70-80ºC.

Subsequently, the so-prepared Pd catalyst power was used to build working electrodes using a similar protocol to that used for the preparation of catalyst coated membranes (CCM) [14]. In more detail, each CCM was manufactured by directly airbrushing the catalytic ink on the membrane and taking into account three main points; a) the evaporation of the solvent in the catalytic layer, b) the elimination of the swelling effect by the solvent in the ink applied and c) a uniform distribution of the catalyst on the membrane. As described in some on our previous contributions [11,12], we have developed a procedure to make catalytic layers, with similar characteristics (morphology and thickness) than those obtained in CCM type electrode architecture, but using gold foils of about 2 cm^2 as current collectors. These gold foils were airbrushed using a catalytic ink containing the Pd electrocatalyst supported on Vulcan XC-72, 5% Nafion as binder and isopropanol (Scharlau, HPLC grade) as a vehicle. For the evaluation the influence of the nominal Pt loading (10, 20, 30 and 40 % wt), the Nafion/total solids ratio as well as Pd catalyst loading were maintained constant to 0.4 and 0.1 mg cm^{-2}, respectively. Similarly, to analyze the influence of the Nafion/total solids ratio (0.05, 0.1, 0.2 and 0.4) the working electrodes were prepared from Pd/C 10% wt and a Pd catalyst loading of 0.1 mg cm^{-2}. Finally, to evaluate the influence of Pd catalyst loading (0.1, 0.5 and 1.2 mg cm^{-2}), the electrodes were fabricated from both 20 and 40 % Pd wt and a Nafion/total solids ratio of 0.4. In this case, the working electrodes were prepared by simply accumulation of layers. In all case, the total evaporation of solvent from catalytic layer was verified by a constant weight after each airbrushing/drying process.

2.2. Physical characterization.

The samples were characterised by Transmission Electron Microscopy (TEM) using a JEOL JEM-2010 microscope working at 200 kV. The sample for TEM analysis was made by depositing a drop of catalyst dispersed in water on a type Formvar copper grid and evaporating to dryness at room temperature. The size distribution and dispersion of the Pd nanoparticles was evaluated by analysing more than 300 nanoparticles from different parts of the grid. Moreover, Scanning Electron Microscopy (SEM, HITACHI S-3000N microscope working at 20 kV) was also employed to analyze both catalytic

layer thickness and morphology of the working electrodes. Catalytic layers were sectioned and scanning electron micrographs of the cross section were obtained and analysed.

2.3 Electrochemical characterization.

The procedure used for the electrochemical characterization of the nanoparticles is similar to that previously reported [11, 12]. In brief, cyclic voltammetry in 0.5 M H_2SO_4 solution was carried out to estimate the electroactive surface area of the electrodes. Electrolyte solutions were daily prepared from Milli-Q® water and Merck ‘‘p.a.” sulphuric acid. Formic acid electrooxidation voltammograms were performed in a 4.75 M HCOOH + 0.5 M H_2SO_4 solution. In addition, chronoamperometric measurements were also carried out at a potential of 0.4 V vs. RHE for 600 s in 4.75 M HCOOH + 0.5 M H_2SO_4 solution. Solutions were prepared from formic acid (Merck ‘‘p.a.’’). All these experiments were performed in a conventional three-electrode electrochemical cell at room temperature. Electrode potential was controlled by a PGSTAT30 AUTOLAB system and all potentials were measured against a reversible hydrogen electrode (RHE) connected to the cell through a Luggin capillary. The counter electrode was a platinum wire. Currents were normalized to the geometric area (two-dimensional surface) of the electrode or to the mass of Pd.

2.4. Breathing direct formic acid fuel cell.

A breathing direct formic acid fuel cell with 6.25 cm^2 was used to test the electrochemical behaviour of the different catalyst coated membranes. The cathode side of membrane was airbrushed with a catalytic ink prepared with a commercially available Pt/C 20 % wt electrocatalyst (HisPEC 3000 Fuel Cell Catalyst, Johnson Matthey). Similarly, the anode side was airbrushed using our so-prepared Pd/C 20 % wt ink. The Pd catalyst loading on the anode side was modified between 0.1, 0.5 and 1.2 mg cm^{-2} whereas the Pt catalyst loading on the cathode side was always 1.0 mg cm^{-2}. A TGPH-090 toray paper (Plain from E-Tek) and a solid polymer electrolyte electrode ELAT (only carbon, 4.5 mg cm^{-2} carbon loading from E-Tek) were respectively employed as “diffusion layers” in the anode and the cathode sides. A single cell was built by pressing catalysts coated membrane and “diffusion layers” between two perforated stainless steel current collectors. A 4.75 M HCOOH + 0.5 M H_2SO_4 solution was fed as fuel at flow rate of 5 mL min^{-1}. The current–voltage curves were recorded using a Solid State Electronic Load ECL 150 system from ElectroChem Inc.

3. RESULTS AND DISCUSSIONS

3.1. Physical and electrochemical characterization of the Pd/C catalysts.

Fig. 1 shows some representative TEM pictures of the samples. As expected, the increase in Pd loading results in a clear particle agglomeration. Thus, whereas for the lowest Pd loading (10 % wt), well-separated 3.5-4.0 nm Pt nanoparticles are clearly discernible, as loading increases, the inter-

nanoparticles distances diminish and a clear particle agglomeration appears. However, it should be pointed out that these aggregates are formed by individual nanoparticles with the same average particle size than those with lower metal loading.

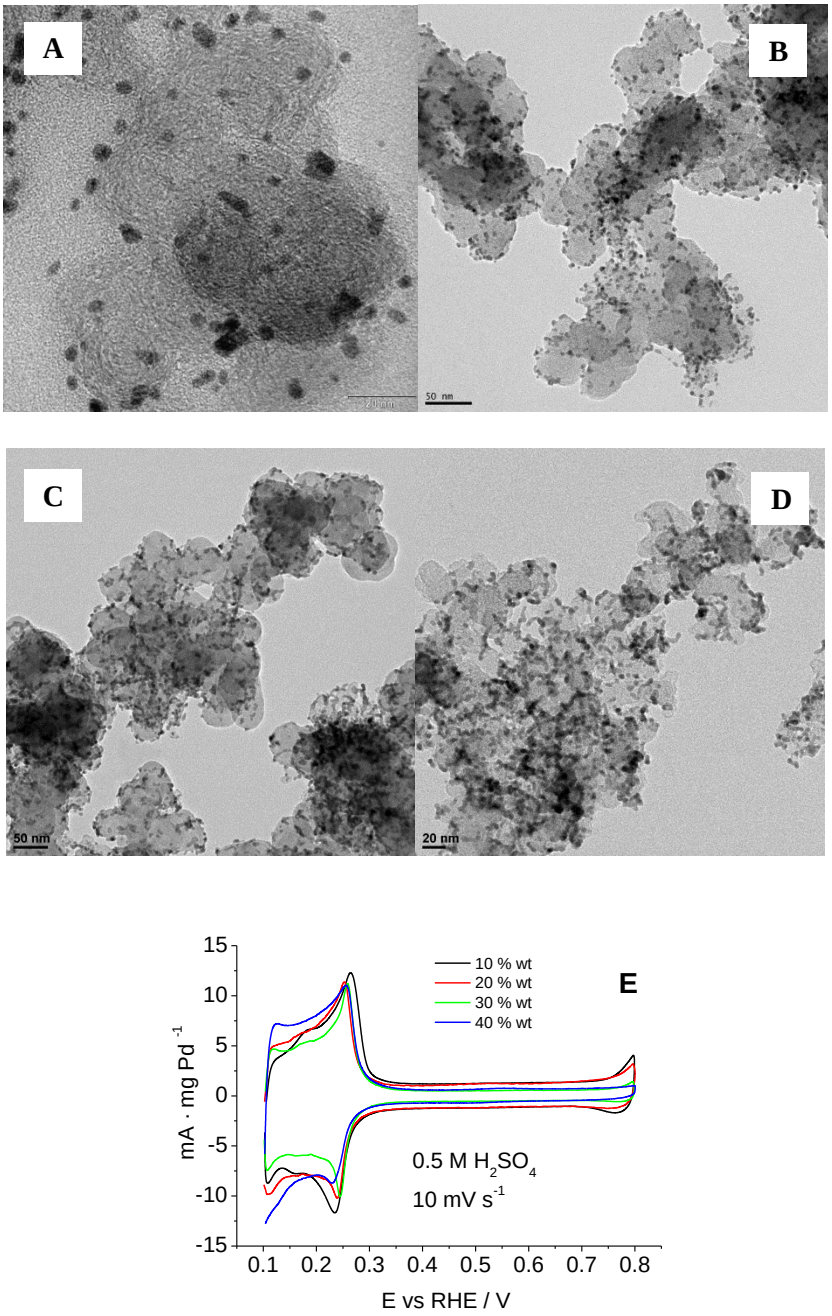

Figure 1. Representative TEM pictures of the carbon supported Pt nanoparticles with different nominal loading, (A) 10, (B) 20, (C) 30 and (D) 40% wt. (E) Characteristic cyclic voltammograms of the samples. Test solution: 0.5 M H_2SO_4, scan rate: 10 mV s^{-1}.

In addition, figure 1E shows the voltammetric response of the different samples obtained in 0.5 M H_2SO_4. All samples show a similar voltammetric feature and characteristic of a polyoriented Pd

surface [15, 16]. Interestingly, when currents are Pd mass normalized as in figure 1E, the voltammograms are in the same current range just showing some variations in the double layer contribution in agreement with the different carbon composition of the electrocatalysts, thus confirming that the samples are formed by Pd nanoparticles with similar properties, in terms of particle size and shape, but with different nominal Pd loading.

Figure 2 reports the electrocatalytic response towards HCOOH electrooxidation obtained with an electrode prepared with the 10 % wt Pd catalyst. The voltammetric response, figure 2A, shows the expected absence of CO-poisoning which is denoted by the good superimposition of the currents in the positive and negative going sweeps. However, during the cronoamperometric experiments a clear current decay is observed which was attributed to the presence of impurities [17, 18] although more recently, Cai et al [19, 20] also evidenced the formation of adsorbed CO poisoning as consequence of the reduction of CO2 in presence of adsorbed hydrogen. In our case, the potential applied is 0.4 V which is high enough to avoid the presence of adsorbed hydrogen thus suggesting that the current decay seems to be related to the presence of impurities a such as high HCOOH concentration.

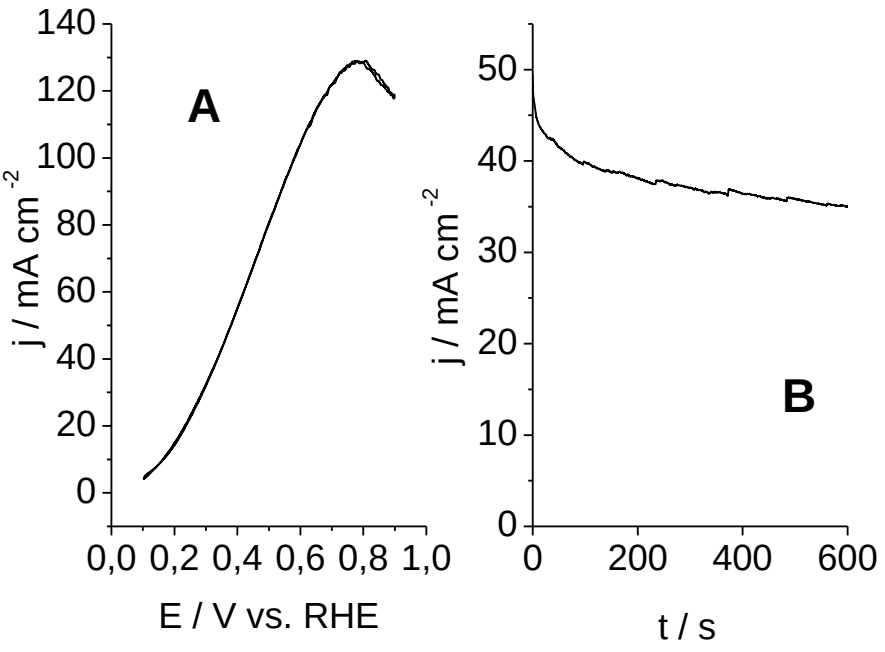

Figure 2. (A) Voltammogram and (B) chronoamperometry at 0.4 V vs. RHE in 4.75 M HCOOH + 0.5 M H_2SO_4 for Pd/C 10 % wt. Pd catalyst loading: 0.1 mg cm^{-2}. Nafion/total solids ratio: 0.4. Scan rate: 10 mV s^{-1}.

3.3. Influence of nominal Pd loading.

To evaluate the effect of the nominal Pd loadings, working electrodes using Pd / C with 10 %, 20 %, 30 % and 40 % Pd wt have been prepared while the other relevant parameters such as the Pd catalyst loading and the Nafion/total solids ratio remained constant at 0.1 mg cm^{-2} and 0.4, respectively. The electrochemical response of the electrodes in 0.5 M H_2SO_4 solution was previously

shown and discussed in figure 1E. Thus, figure 4 shows the current-time responses of the electrodes obtained at 0.4 V vs. RHE in 4.75 M HCOOH + 0.5 M H_2SO_4 solution. No significant variations in the formic acid electrooxidation currents, normalised to the geometric area of the electrodes, have been found for different nominal weight percentages of Pd although a slight improvement can be observed with increasing Pd % wt in the catalytic layer. It is important to note that due to the low Pd catalyst loading (0.1 mg cm^{-2}), the differences on the catalytic layer thickness are not very important ranging between 3 and 4 microns. The effect of the catalytic layer thickness will be described in more detail in a forthcoming section.

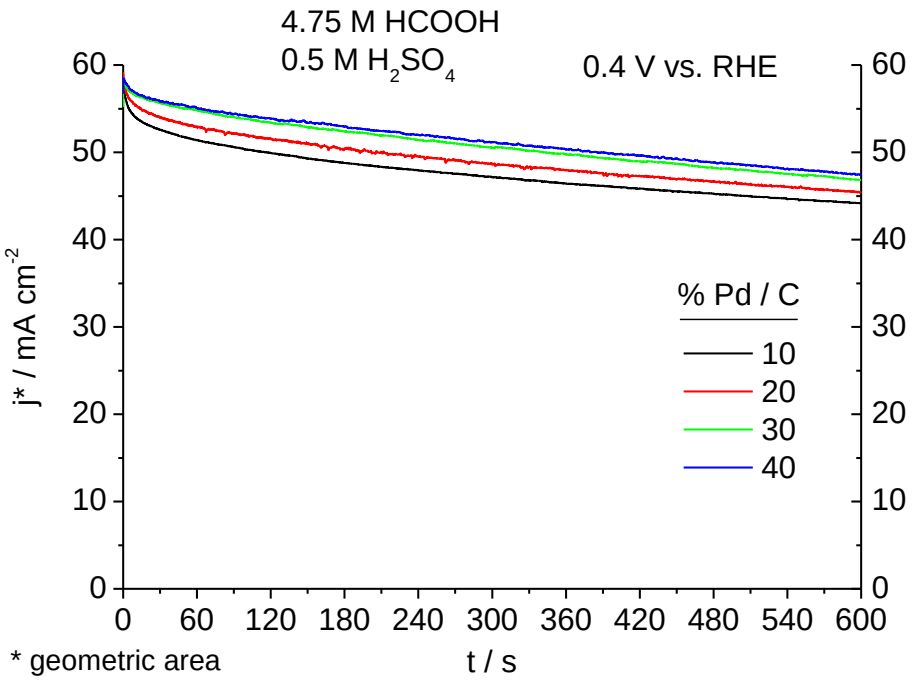

Figure 3. Chronoamperometric measurements recorded at 0.4 V vs. RHE. in 4.75 M HCOOH + 0.5 M H_2SO_4 for different nominal Pd loadings. Nafion / total solids ratio of 0.4 and Pd catalyst loading of 0.1 mg cm^{-2}.

3.3. Influence of the Nafion / total solids ratio.

In this section we have evaluated the possible influence of the percentage of Nafion, expressed as Nafion/total solids ratio on the electrocatalytic properties. Different working electrodes with a Nafion/ total solids ratio of 0.05, 0.1, 0.2 and 0.4 were prepared while the other parameters were kept constant (nominal loading Pd/C 10% wt and Pd catalyst loading 0.1 mg cm^{-2}). The voltammetric profiles obtained in 0.5 M H_2SO_4 were, as expected, almost identical. In addition, in chronoamperometric experiments at 0.4 V vs. RHE in 4.75 M HCOOH + 0.5 M H_2SO_4 solution, no significant changes were again observed for increasing Nafion/total solids ratios. Note that, for the Nafion/total solids ratio of 0.05, the catalytic layer showed a bad cohesion during the electrochemical

characterization thus being impossible evaluating its electrocatalytic analysis. Based on the reported results, under these conditions (environmental conditions), Nafion only acts as a structural agent of the catalytic layer without a relevant influence on their electrocatalytic properties.

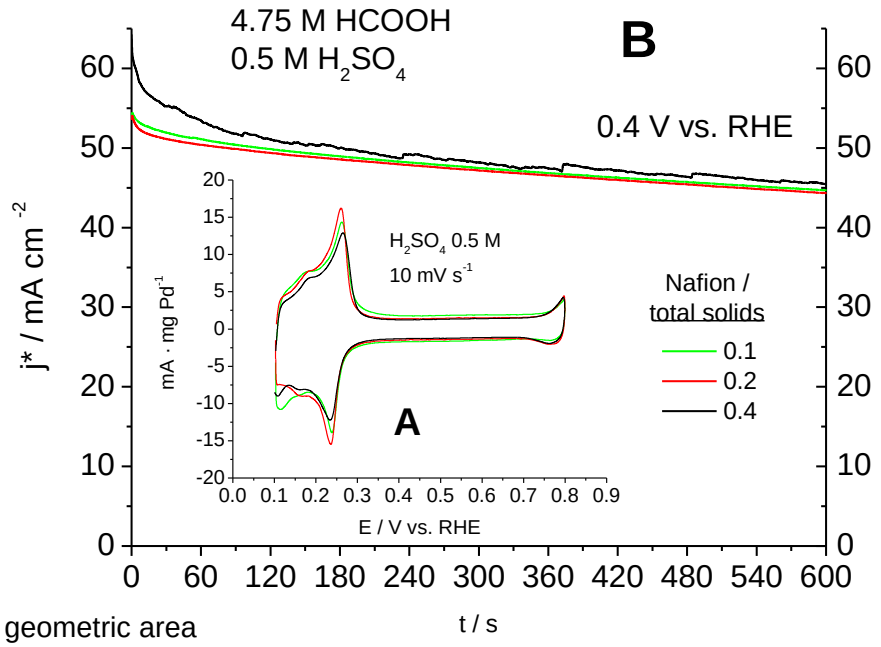

Figure 4. Influence of the ratio Nafion/total solids on the (A) voltammetric response obtained in 0.5 M H_2SO_4, scan rate 10 mV s^{-1} and on the (B) formic acid electrooxidation current/ time response at 0.4 V vs. RHE in 4.75 M HCOOH + 0.5 M H_2SO_4. Nominal Pd loading: Pd/C 10 % wt. Pd catalyst loading: 0.1 mg cm^{-2}.

3.4. Influence of the catalyst loading on the catalytic layer.

To determine the influence of the Pd loading on the catalytic layer, different working electrodes with Pd catalyst loading of 0.1, 0.5 and 1.2 mg cm^{-2} were prepared using two different nominal Pd loading (Pd/C 20 % and 40 % wt). In all cases, the Nafion/total solids ratio was maintained to 0.4. The voltammetric response of these working electrodes was again obtained in 0.5M H_2SO_4 solution showing similar features to those shown in figures 1e and 4a. Figures 5 and 6 show the electrocatalytic behaviour towards formic acid electrooxidation, where currents were normalized to geometric area of the electrodes, for the different electrodes. These results clearly indicate that the increase of the Pd loading does not result in a benefit proportional to the increase of loading. Thus, whereas the loading is multiplied by 10, the current is only improved about twice thus suggesting an important decrease on the Pd utilization. These results are in good agreement with some of our previous observations [11, 12]. To complete this picture, we have also analysed the thickness of the catalytic layer of each one of the working electrodes by cross-section SEM micrographs (figure 7).

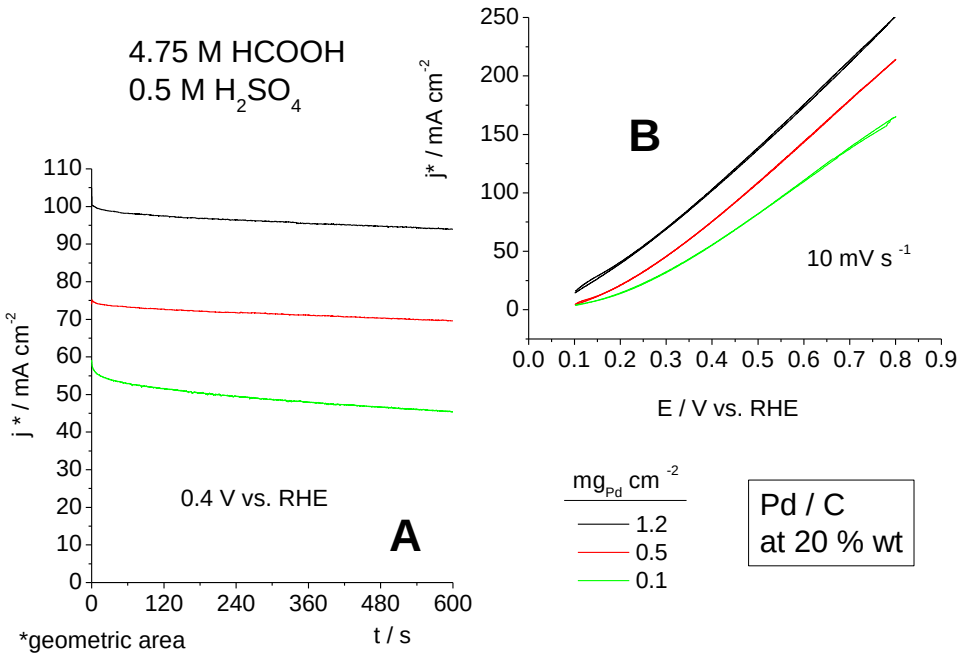

Figure 5. Influence of the Pd loading for nominal Pd loading of 20 % wt in (A) chronoamperometric measurements at 0.4 V vs. RHE in 4.75 M HCOOH + 0.5 M H_2SO_4 and in (B) voltammogramsn in 0.5 M H_2SO_4. Scan rate 10 mV s^{-1}. Nafion / total solids ratio 0.4.

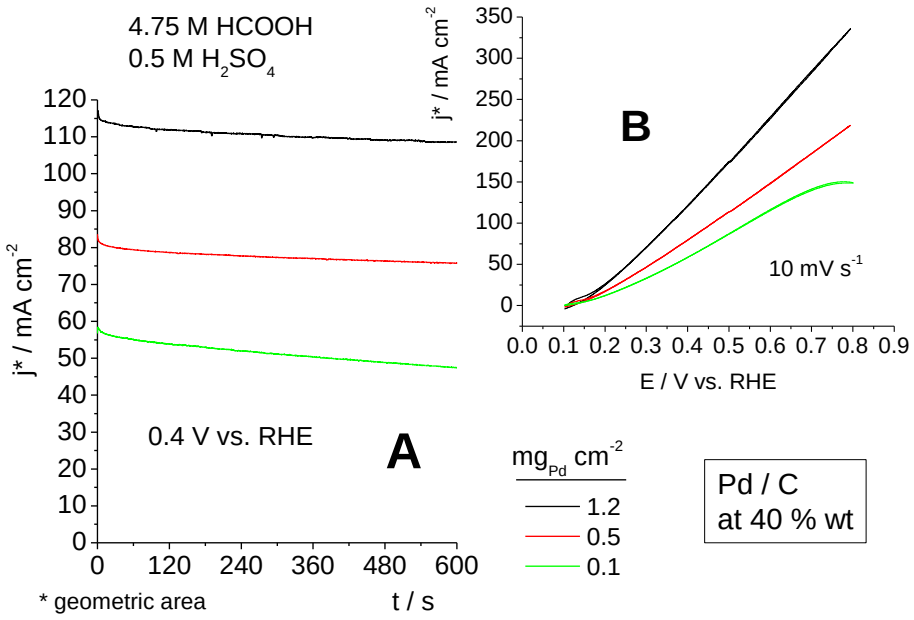

Figure 6. Influence of the Pd loading for nominal Pd loading of 40 % wt in (A) chronoamperometric measurements at 0.4 V vs. RHE in 4.75 M HCOOH + 0.5 M H_2SO_4 and in (B) voltammogramsn in 0.5 M H_2SO_4. Scan rate 10 mV s^{-1}. Nafion / total solids ratio 0.4.

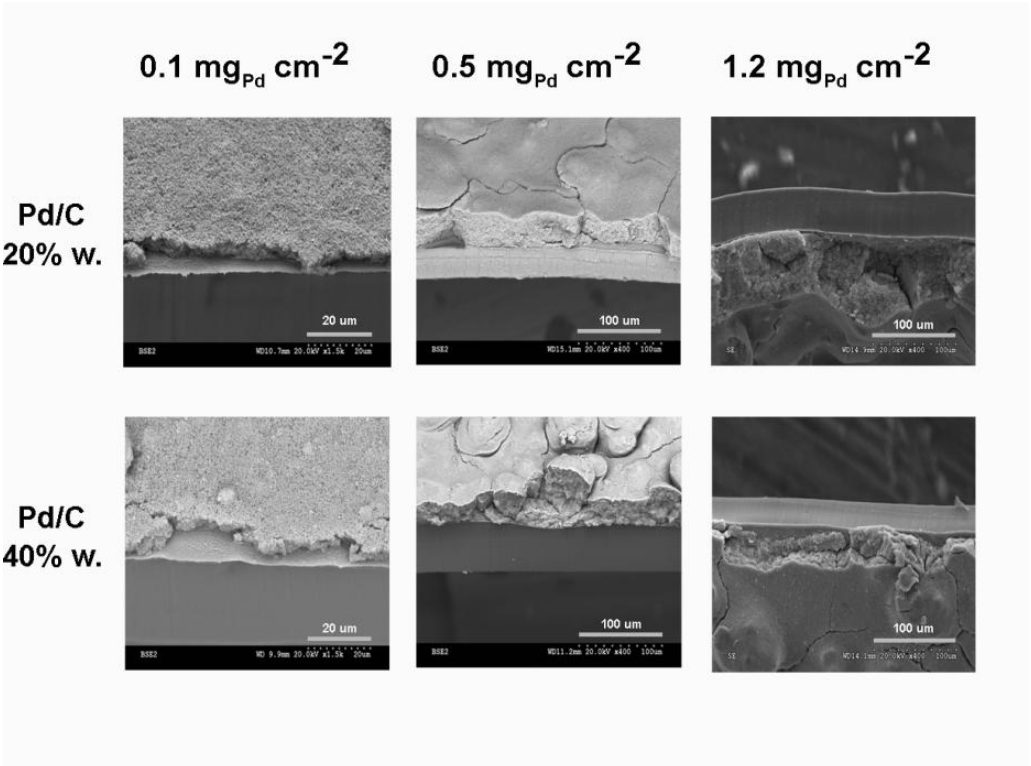

Figure 7. Cross-section SEM micrographs of the catalytic layers with Pd catalyst loadings of 0.1, 0.5 and 1.2 mg cm^{-2} using Pd/C 20 % and 40 % wt. Nafion / total solids ratio: 0.4.

Table I reports the current normalized geometric area current densities recorder after 600s at 0.4 V in 4.75 M HCOOH + 0.5 M H_2SO_4, figures 5A and 5B, as well as the catalytic layer thickness of each electrode. Some important features should be noted. As expected, independently of the nominal Pd loading used, when the catalytic loading is increased, by simply accumulation of layers, an increase in the catalytic layer thickness is observed. However, this increasing thickness is much higher for low nominal Pd loading due to the much higher amounts of carbon. In addition, this increasing thickness is most pronounced from 0.1 mg cm^{-2} to 0.5 than from 0.5 to 1.2. Nevertheless, the most interesting point is that the electrooxidation currents seem to be almost independent of the thickness.

Table 1. Normalized geometric area current densities obtained from figure 5A and 6A and their corresponding catalytic layer thickness.

	j / mA cm^{-2}			**Aprox. thickness (μm)**		
Pd catalyst loading / mg cm^{-2}	**0.1**	**0.5**	**1.2**	**0.1**	**0.5**	**1.2**
20 % wt	46	71	96	4	40	80
40 % wt	47	75	106	4	20	40

Thus, for instance, for electrodes with a catalyst loading of 0.5 mg cm^{-2}, whereas the thickness is 40 and 20 μm for electrodes prepared from 20 and 40 % wt, respectively, the electrooxidation currents are almost similar about 70-75 mA cm^{-2} thus indicating the low impact of the thickness and

suggesting that the amount of Pd in the outer layer is the key parameter determining their electrocatalytic properties. This fact also implies that, from the point of view of Pd utilization, those electrodes having smaller thickness will more efficiently use the Pd electrocatalysts.

3.5. Polarization curves in breathing direct formic acid fuel cell.

With the information acquired in the previous sections with the gold supported catalytic layer, catalyst coated membranes with different Pd loading were manufactured (CCM). These CCM were prepared following the details described in the experimental section. Figure 8 shows the polarization and power curves obtained with the different CCMs. The results obtained with metal loading of 0.5 and 1.2 mg cm^{-2} are similar to those previously shown in the literature [21, 22] and comparable with those obtained with the gold supported catalytic layer approach with similar Pd loadings. Nevertheless, the performance observed with the CCM containing a Pd catalyst loading of 0.1 mg cm^{-2} is unexpectedly low and far from the values obtained with the gold supported electrodes.

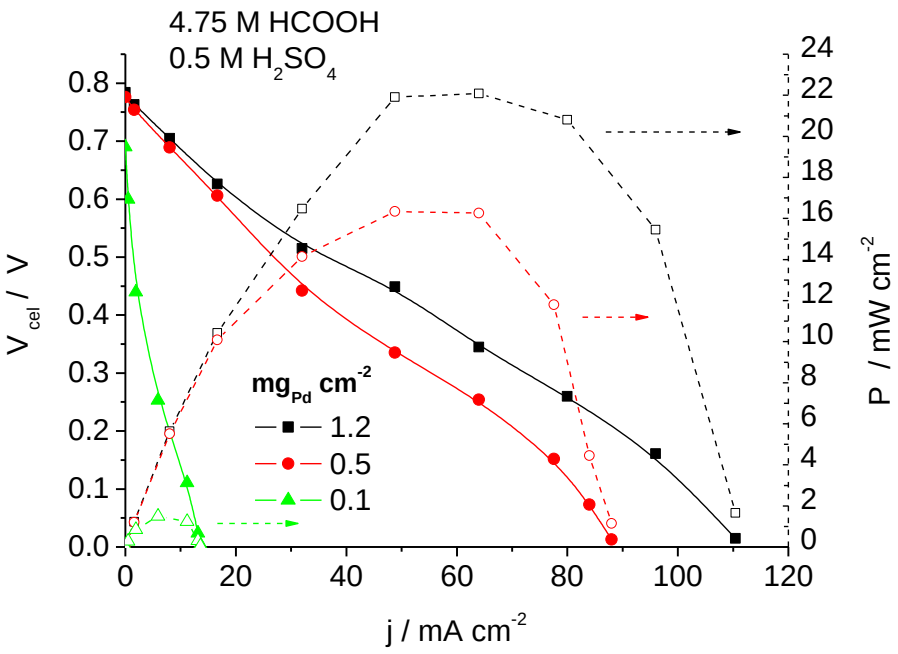

Figure 8. Polarization curves in a breathing direct formic acid fuel cell. Catalyst-coated membrane: 1) Cathode: Pt/C 20% wt (HisPEC 3000 Fuel Cell Catalyst, Johnson Matthey) with Pt catalyst loading of 1.0 mg cm^{-2}, 2) Anode: Pd/C 20 % wt (same using in working electrode experiences) with Pd catalyst loading of 0.1, 0.5 and 1.2 mg cm^{-2}. Nafion / total solids ratio: 0.4. Configuration of breathing fuel cell system was a catalyst coated membrane between electrode type ELAT (Vulcan XC-72 loading of 4.5 mg cm^{-2}) as cathodic diffusion system and Toray paper TGPH-90 as anodic diffusion system. Fuel used was 4.75 M HCOOH in 0.5 M H_2SO_4 at a flow rate of 5 mL min^{-1}.

The low performance of the catalyst coated membrane containing a Pd catalyst loading of 0.1 mg cm^{-2} could be due to a poor electric contact between the catalytic layer and the current collector

backing layer. To verify this hypothesis some new experiments were carried out in which an additional layer prepared from Vulcan XC-72, Nafion 5 %, isopropanol and a Nafion / total solids ratio of 0.4 was airbrushed both between the membrane and the catalytic layer and between the catalytic layer and the current collector backing layer. The final amount of Vulcan XC-72 on the new layer was the same as the catalyst coated membrane with a Pd catalyst loading of 1.2 mg cm^{-2} (20% wt and thickness of 80 microns - see table 1 -). Figure 9 shows the results obtained with these modified systems. Interestingly, when the new layer is in between the membrane and the catalytic layer, the performance of the system is clearly improved whereas the performance gets worse when the new layer is in between the catalytic layer and the current collector backing layer. This fact suggests that when the carbon layer is between the membrane and the catalytic layer, not only the electric contact is improved but also the Pd layer utilization. In fact, when the carbon layer is between the catalytic layer and the backing layer and despite a similar electric contact improvements should take place, the performance is worse as consequence of limitations in the accessibility of the fuel, trough the carbon layer, to the catalytic one. However, the improved performance is still limited and more work is in progress to optimize it. These results evidence that the current density values obtained with the gold supported electrodes come from a direct interaction between the catalytic layer and the fuel without taking into account other design parameters of relevance on the performance of a breathing direct formic acid fuel cell.

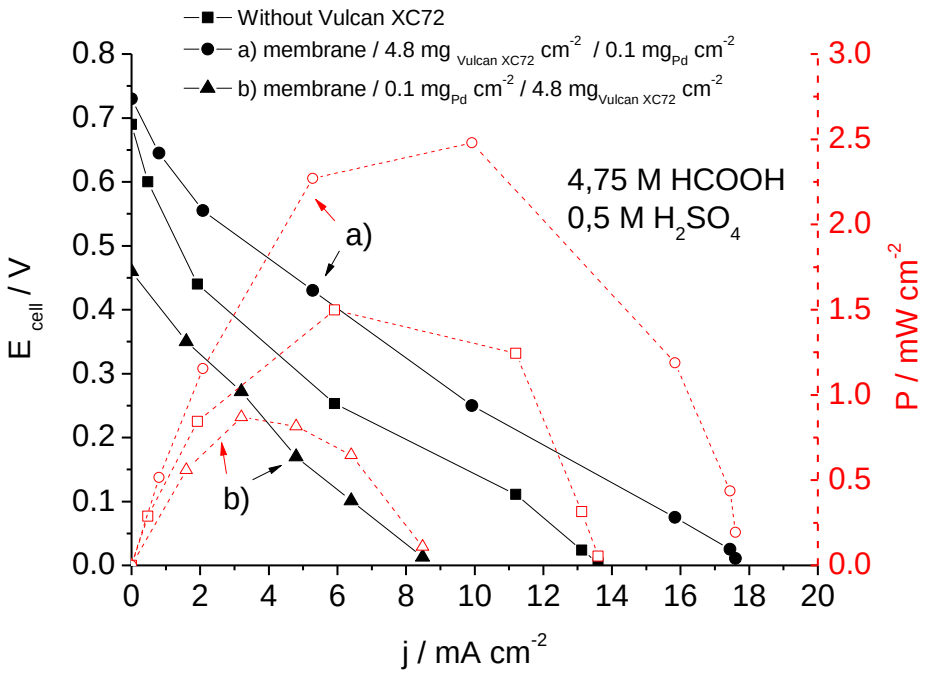

Figure 9. Comparison of polarization curves of three catalyst coated membranes by a Pd catalyst loading of 0.1 mg cm^{-2}. ■: without modification of the catalytic layer; ●: modification of the catalytic layer by increasing thickness with the same amount of Vulcan XC-72 in a Pd catalyst loading of 1.2 mg cm^{-2}, catalytic layer: membrane / Vulcan XC-72 loading of 4.8 mg cm^{-2} / Pd catalyst loading of 0.1 mg cm^{-2}; ▲: modification of the catalytic layer by increasing thickness with the same amount of Vulcan XC-72 in a Pd catalyst loading of 1.2 mg cm^{-2}, catalytic layer: membrane / Pd catalyst loading of 0.1 mg cm^{-2} / Vulcan XC-72 loading of 4.8 mg cm^{-2}.

4. CONCLUSION

Formic acid electrooxidation on Vulcan XC-72 supported Pd nanoparticles was evaluated from gold supported electrodes to catalyst-coated membranes. The use of gold supported electrodes allowed us to determine the influence of important parameters in the construction of the catalytic layer such as the Nafion / total solids ratio, the nominal percentage of Pd on Vulcan XC-72 as well as the different Pd loadings on the resulting electrocatalytic activity. The results obtained suggest that whereas almost no influence is found for different Nafion / total solids ratio and different nominal Pd loading (10 - 40 %wt), the activity is mainly determine by the Pd loading on the catalytic layer. However, the results also indicate that the increase of the Pd loading does not produce a current density proportional to the increase of loading. This fact implies an important decrease on the Pd utilization and also suggests a low impact of the catalytic layer thickness. Consequently, the resulting electrocatalytic properties are mainly determined by the amount of Pd in the outer layer of the catalytic layer.

Finally catalyst coated membranes with anode Pd catalyst loadings of 0.1, 0.5 and 1.2 mg cm^{-2} and cathode Pt catalyst loading of 1.0 mg cm^{-2} have been tested in a breathing direct formic acid fuel cell. A good correlation between the results obtained with the gold supported electrodes and those obtained in the polarization curves were found for Pd catalyst loadings of 0.5 and 1.2 mg cm^{-2}. Nevertheless, in case of lower Pd catalyst loading (0.1 mg cm^{-2}), important discrepancies were observed which seems to be related to a poor electric contact of the catalytic layer. In fact, an improvement is observed when a layer of Vulcan XC-72 is interposed between the membrane and the catalytic layer. More work is in progress to optimize the electrocatalytic behaviour of the CCM in the low Pd catalyst loading region.

ACKNOWLEDGEMENTS
This work has been financially supported by the Ministerio de Ciencia e Innovación of Spain through project CTQ2010-20347.

References

1. L. Zhang, Y. Tang, J. Bao, T. Lu, C. Li, *J. Power Sources*, 162 (2006**)** 177
2. M. Weber, J.T. Wang, S. Wasmus, R.F.J. Savinell, *J. Electrochem. Soc*. 143 (1996) L158
3. C. Rice, S. Ha, R.I. Masel, P. Waszczuk, A. Wieckowski, T. Barnard, *J. Power Sources*, 111 (2002) 83
4. C. Rice, S. Ha, R.I. Masel, A. Wieckowski, *J. Power Sources*, 115 (2003**)** 229
5. A. Capon, R. Parsons, *J. Electrroanal. Chem.*, 44 (1973) 1.
6. A. Capon, R. Parsons, *J. Electroanal. Chem.*, 45 (1973) 205.
7. M.J. Llorca, J.M. Feliu, A. Aldaz, J. Clavilier, *J. Electroanal. Chem.*, 376 (1994) 151.
8. J. Solla-Gullón, V. Montiel, A. Aldaz, J. Clavilier, *J. Electrochem. Soc.*, 150 (2003) E104.
9. G. Q. Lu, A. Crown, A. Wieckowski, J. Phys. Chem. B, 103 (1999) 9700.
10. R. S. Jayashree, J. S. Spendelow, J. Yeom, C. Rastogi, M. A. Shannon, P. J. A. Kenis, Electrochim. Acta, 50 (2005) 4674.
11. A. Sáez, E. Expósito, J. Solla-Gullón, V. Montiel, A. Aldaz, *Electrochim. Acta*, 63 (2012) 105.
12. A. Sáez, J. Solla-Gullón, E. Expósito, V. Montiel, A. Aldaz, *Electrochim. Acta*, 54 (2009) 7071
13. J. Solla-Gullón, A. Rodes, V. Montiel, A. Aldaz, J. Clavilier, *J. Electroanal. Chem.* 273 (2003) 554

14. R. R. Passos, V. A. Paganin, E. A. Ticianelli, *Electrochim. Acta*, 51 (2006) 5239
15. L. D. Burke, L. C. Nagle, *J. Electroanal. Chem.*, 461 (1999) 52.
16. F.J. Vidal-Iglesias, R.M. Arán-Ais, J. Solla-Gullón, E. Garnier, E. Herrero, A. Aldaz, J.M. Feliu, *Phys. Chem. Chem. Phys.*, 14 (2012) 10258.
17. W. L. Law, A. M. Platt, P. D. C. Wimalaratne, S. L. Blair, *J. Electrochem Soc.* 156 (2009) B553.
18. X. Zhang, H. Galindo, H. Garces, P. Baker, X. Wang, U. Pasaogullari, S. Suib, T. Molter, *J. Electrochem. Soc.* 157 (2010) B409.
19. H.-X. Zhang, S.-H. Wang, K. Jiang, T. André, W.-B. Cai, J. Power Sources, 199 (2012) 165.
20. J.-Y. Wang, H.-X. Zhang, K. Jiang, W.-B Cai, J. Am. Chem. Soc., 133 (2011) 14876.
21. S. Ha, B. Adams, R. I. Masel, J. Power Sources, 128 (2004) 119
22. P. Hong, S. Liao, J. Zeng, X. Huang, J. Power Sources, 157 (2011) 78